AEGC2019 Data to Discovery
Australasian Exploration Geoscience Conference
2-5 September 2019 • Perth, Western Australia
Incorporating the AIG, ASEG, PESA, and WABS

Observations of geophone spurious resonance

Steve Hearn*
Velseis Pty Ltd and University of Qld.
steveh@velseis.com

Shaun Strong
Velseis Pty Ltd
sstrong@velseis.com

Andrew Kinmont
Sapiens Innovations
andrew.kinmont@live.com.au

SUMMARY

A detailed understanding of the frequency response of geophones is critical for the design and quality control of broadband seismic surveys. We illustrate a pragmatic methodology for accurate identification of geophone spurious resonances. We include tap-test examples from conventional 10 Hz geophones, and from 5 Hz and 10 Hz high-output nodal sensors. High-frequency noise sources, including high-voltage harmonics can interfere with the accurate identification of the spurious events. This problem can be overcome by subtraction of matched noise spectra

Key words: broadband, geophone, resonance, spurious frequency

INTRODUCTION

The electrodynamic geophone has arguably been one of the most important instrumental contributors to the seismic industry. The fact that this analogue sensor has persisted for many decades is a tribute to classic design. The operation of the geophone is now well understood. At the low-frequency end, the response typically rolls off at 12 dB/octave, commencing at the natural frequency (3 dB down in a typically damped device). Currently there is significant industry interest in extending the recording bandwidth to lower frequencies, with a corresponding global trend towards geophones having lower natural frequencies. For decades, the 10 Hz geophone has been the standard, with 5 Hz sensors now also being used, particularly in nodal systems.

At the high-frequency end, the geophone theoretically has response beyond the range of recovered frequencies. In practice the high-frequency response is affected by secondary resonances generally associated with motions other than the primary on-axis coil movement. These have commonly been referred to as spurious or parasitic resonances. Given the fundamental nature of the sensor in the recording chain, there has been relatively little recent analysis in the literature. Important earlier investigations include Chen and Dalton (1983) and Faber and Maxwell (1997).

Geophone manufacturers are generally concise in their specification of spurious resonance, often quoting a nominal lower limit for any spurious responses. This may relate to the possibility of manufacturing variability. Seismic survey design would benefit from more detailed specification of resonance parameters. Laboratory-based analysis is relatively straightforward (e.g. Faber and Maxwell, 1997) but requires specially constructed test equipment.

The main purpose of this paper is to illustrate a fairly simple practical approach to identifying the precise frequencies at which spurious activity occurs. This information is critical when considering Vibroseis sweep ranges. We include example observations from 10 Hz (385 Ω) conventional geophones, and from 5 Hz (1850 Ω) and 10 Hz (1800 Ω) high-output nodal sensors. The simple tests described here could potentially be carried out on any seismic crew.

TAP-TEST METHODOLOGY

Our main experiments were carried out with a standard tap-test approach, with a repetitive sequence of taps applied to various parts of the sensor. We experimented with various tapping utensils. The results shown here were achieved using a small wooden survey peg. Typically, each individual record was around eight seconds, incorporating about five or six taps. We attempted to apply a sharp, but relatively low-energy tap, monitoring the record to ensure no clipping occurred. We used a high-quality 32 bit ADC system. Inconsistent taps were obvious on the records, and were excluded.

Figure 1 shows a typical tap record, for a conventional 10 Hz geophone, planted vertically. The main event is very strong, with no immediate evidence of associated resonances. The typical tap spectrum is broadband (Figure 2, top). There is often some evidence of small distortions (< 1 dB) in the spectrum at higher frequencies, although it is not necessarily apparent whether these are instrumental or related to external noise sources (Figure 2 bottom).

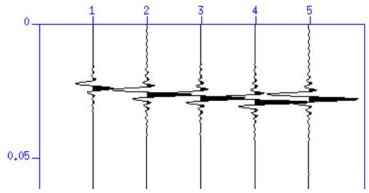

Figure1. Example signatures for vertical 10 Hz geophone tapped on top.

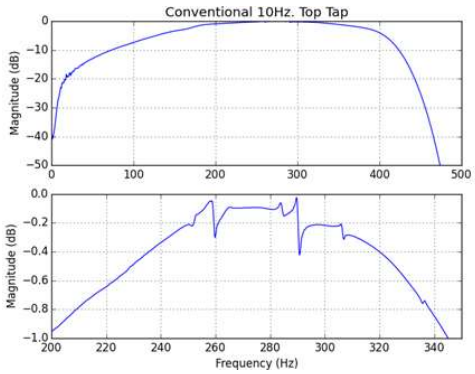

Figure 2. (Top) Average spectrum of full traces (1.024s) corresponding to Figure 1. (Bottom) Zoom: 200 to 350 Hz, 0 to -1 dB.

Following the approach of Faber and Maxwell (1997), clearer evidence of spurious activity is obtained by examining a window following each tap event. In our experiments we achieved good results using an analysis window of length between 0.5s and 1.0s, and starting about 0.1s - 0.2s after the main tap. Figure 3 shows the analysis window corresponding to the data in Figure 1, amplified to reveal various low-level noise, possibly including spurious resonance. Figure 4 shows the corresponding average spectrum, in dB and linear formats. The latter is the natural domain for noise subtraction, and is also convenient for highlighting spectral peaks.

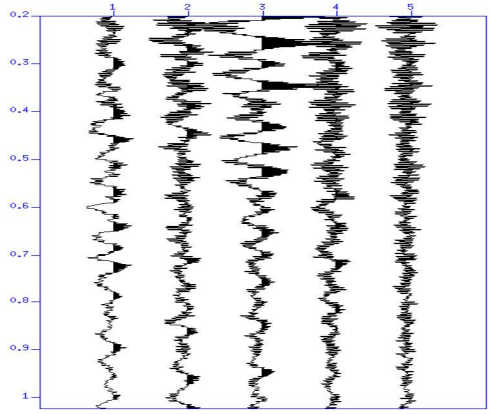

Figure 3. Analysis window (0.2 – 1.0 s) following the taps in Figure 1.

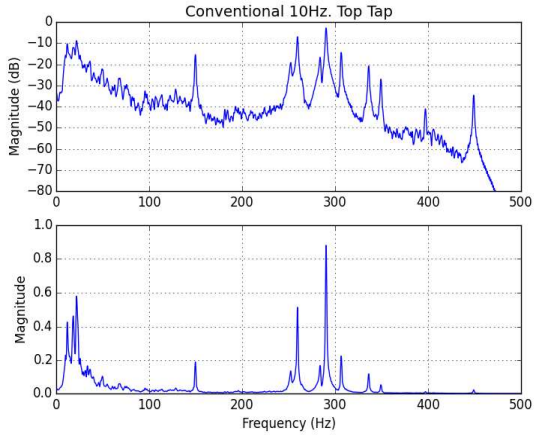

Figure 4. Average spectrum of the trace segments in Figure 3, shown in dB (top) and normalised magnitude (bottom).

SPECTRAL NOISE SUBTRACTION

In the particular location of our tests, we found that the low-amplitude analysis window was contaminated with various noise events, including high-voltage odd harmonics often visible at 150 Hz, 250 Hz, 350 Hz and 450 Hz. These have a spectral signature not unlike that from spurious resonance, and hence could easily be misinterpreted as such. (Following full analysis we found that some of these high-voltage peaks were located very close to real resonance peaks.) Spectral noise subtraction is standard practice in related disciplines where low-amplitude events are being sought in a potentially noisy environment. Such applications include acoustics (e.g. Boll, 1979) and medical imagery (e.g. Erturk et al., 2013).

We recorded an eight-second noise record prior to, and after, each tap sequence. The noise was segmented to match the data, and processed to yield an average noise spectrum matching the data in terms of resolution and amplitude.

Figure 5 gives a typical example of the spectral subtraction process, for a case where various noise sources are present, including low-frequency noise (mainly road noise) and high-voltage peaks. Importantly, the process allows visual QC of which peaks are noise related. With the matching process used, noise harmonics can be effectively attenuated even from underneath coincident resonance peaks. In the following analyses, matched-noise subtraction has been applied to each spectrum.

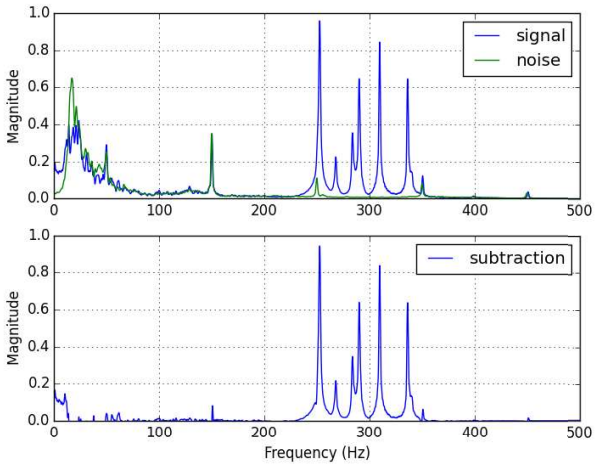

Figure 5. Typical example of matched-noise subtraction, showing attenuation of low-frequency background noise and high-voltage noise spikes at 50, 150, 250, 350 and 450 Hz.

TILT EXPERIMENTS

An initial series of tilt experiments were performed with a conventional 10 Hz geophone, and with 10 Hz and 5 Hz high-output nodal sensors. Illustrative results are included here. Our primary interest is in the frequencies of resonances, and these are considered meaningful to within about 1-2 Hz. Resonance amplitudes are certainly affected by inconsistent tap strength, and should be treated more qualitatively. However, we have examined the amplitude effects closely and believe the major amplitude variations observed in spectra indicate true variations in resonance.

Figure 6 examines the conventional 10 Hz geophone. It compares the response to top and side impacts, for vertical plants and several tilted cases. For a vertical plant (top plot) there are six strong spurious resonances beginning at around 250 Hz (252, 259, 284, 290, 306, 336 Hz). These occur for both top and side taps, although the relative strengths change for different tap orientations. The resonance frequencies do not change significantly with tap orientation. The spectral positions are generally maintained for a tilt of 12°, suggesting that the resonance frequencies are consistent over the range of 'acceptable' geophone plants. Even at 26° tilt the main peak frequencies are reasonably stable, although some new smaller peaks emerge. For extreme tilts (45°) peak frequencies are reduced significantly, and peak magnitudes decrease.

Figure 7 shows the same analysis for a 10 Hz nodal sensor. A simpler resonance pattern is apparent. For vertical plants there are strong resonances around 280 Hz and 335 Hz, with a weak peak at 310 Hz.

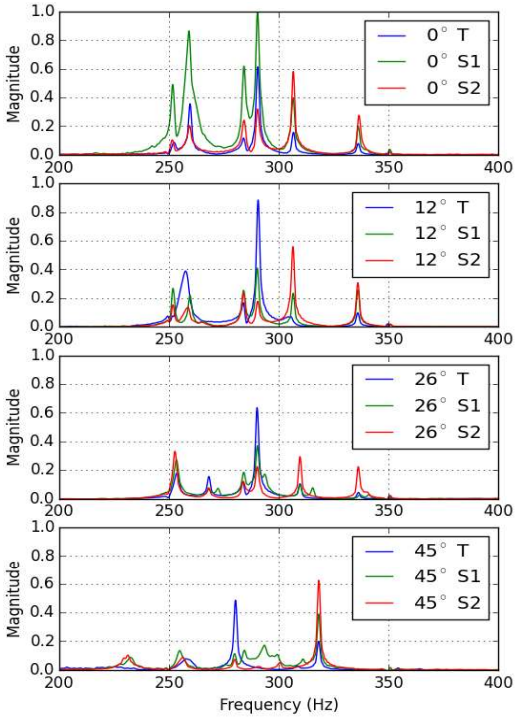

Figure 6. Example of noise-subtracted average spectra for a conventional 10 Hz geophone. From top to bottom: Vertical plant, 12°, 26°, 45° tilt. Each plot includes results for top taps (blue) and orthogonal side taps (green, red).

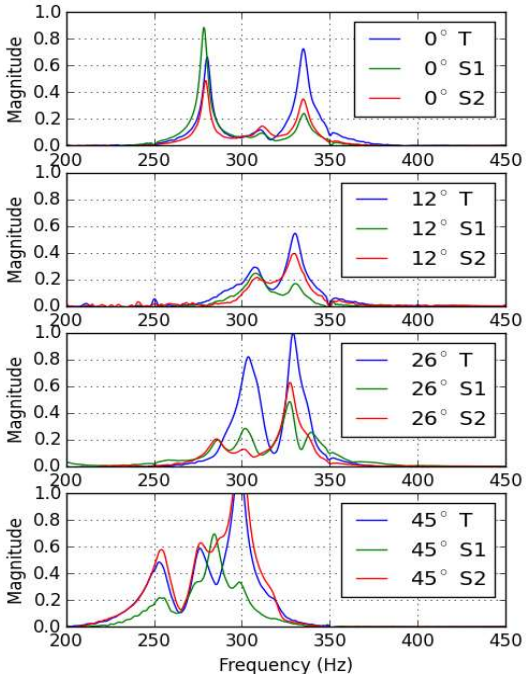

Figure 7. Noise-subtracted average spectra for 10 Hz nodal sensor. From top to bottom: Vertical plant, 12°, 26°, 45° tilt. Top taps (blue) and orthogonal side taps (green, red).

Interestingly, the lower-frequency peak does not appear for the 12°tilt, while the 310 Hz peak becomes more prominent. For more severe tilts (26°, 45°), frequencies decrease, and resonance becomes stronger.

The 5 Hz nodal sensor exhibited a very simple resonance pattern (Figure 8). The vertical plant shows a single strong resonance at 186 Hz, while for a 12° plant the resonance is stronger, and its frequency drops slightly (183 Hz). For more severe tilt (26°) the resonance frequency drops significantly and a second peak emerges. For extreme tilt (45°), the resonance appears to be severely damped.

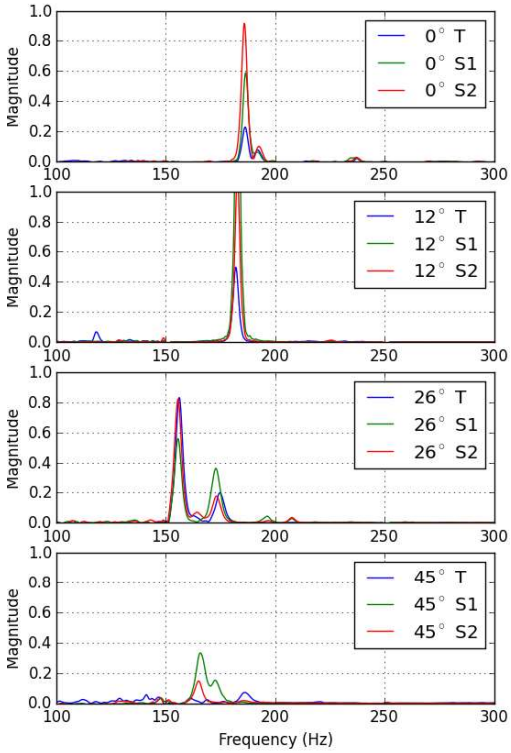

Figure 8. Example of noise-subtracted average spectra for 5 Hz nodal sensor. From top to bottom: Vertical plant, 12°, 26°, 45° tilt. Top taps (blue) and orthogonal side taps (green, red).

In all the tests above, resonances were stimulated by both top and side impacts, suggesting that any wave type could potentially cause the behaviour. In addition, the direction of side impact can affect the resonance behaviour, at least in magnitude. Hence, observed resonance might depend on variable positioning of elements in cases. Azimuthal variation is obviously also significant in 3D surveys. To further explore this effect, we carried out more detailed directional testing.

AZIMUTHAL EXPERIMENTS

Figure 9 shows spectra from a set of azimuthal tests on a conventional 10 Hz geophone, planted vertically. Importantly, the lowest frequency peak (252 Hz) is very stable with respect to impact azimuth, as are Peaks 3,4,5,6. Peak 2 (nominally 259 Hz) appears to drop by several Hz at particular azimuths. Figure 10 details these changes in peak frequency and magnitude for the two lower frequency resonances. For these two peaks, the magnitude variation around the mean is of

order 5 dB, and appears somewhat cyclic. This may possibly relate to the coil suspension mechanism.

Figure 11 summarises the azimuthal variations in the two peaks for a vertically planted 10 Hz nodal geophone. In this case both resonance frequencies are stable (to about 1 Hz) with respect to impact azimuth, while magnitude again varies by 5 dB around the mean.

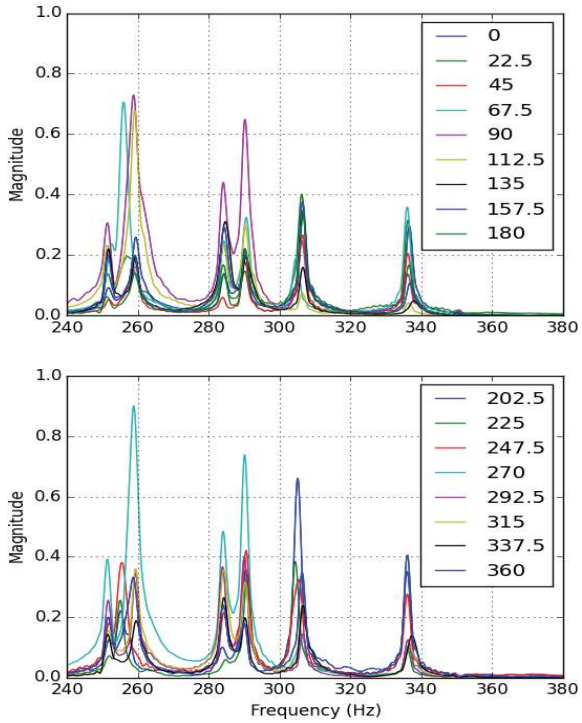

Figure 9. Conventional 10 Hz geophone: Noise-subtracted spectra for impact azimuths at 22.5° increments (legend).

Figure 12 summarises the azimuthal variations in the single peak for a vertically planted 5 Hz Nodal geophone. Frequency is stable (to about 2 Hz) with respect to impact azimuth, while magnitude variation is of order 10 dB around the mean.

FIELD EXPERIMENT

We performed a short field experiment, aimed at exciting spurious resonance in the high-output nodal sensors. During a 2D production Vibroseis survey, we substituted four conventional 10 Hz geophones with nodal sensors. A pair of nodal sensors (5Hz and 10 Hz) were place at relatively near offset (approximately 100m) and another pair were placed at intermediate offset (around 500m).

We were primarily exploring the response of the 5 Hz sensor, so we executed sweeps (20-180 Hz) which ended just below the expected resonance (~186 Hz), and other sweeps which extended past the expected resonance (20-200 Hz, 20-220 Hz). Close examination revealed no evidence of spurious behaviour on any parts of the nodal traces (or on the conventional geophones).

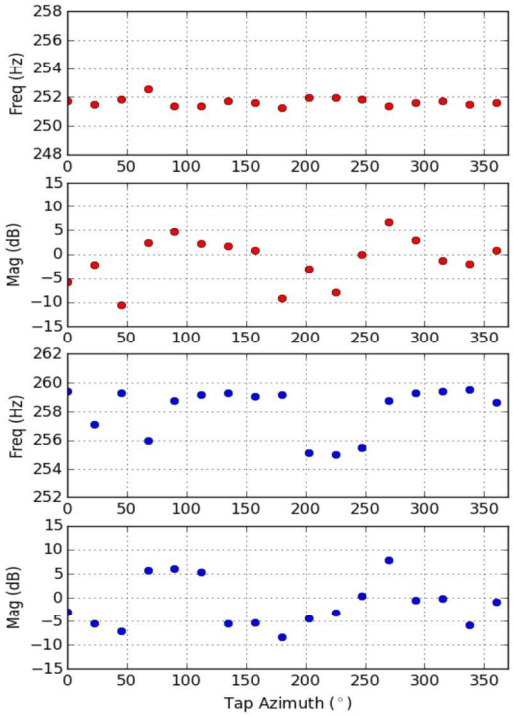

Figure 10. Azimuthal variation in frequency and magnitude for Peaks 1 and 2 from Fig 9. (252 Hz, red; 259 Hz, Blue)

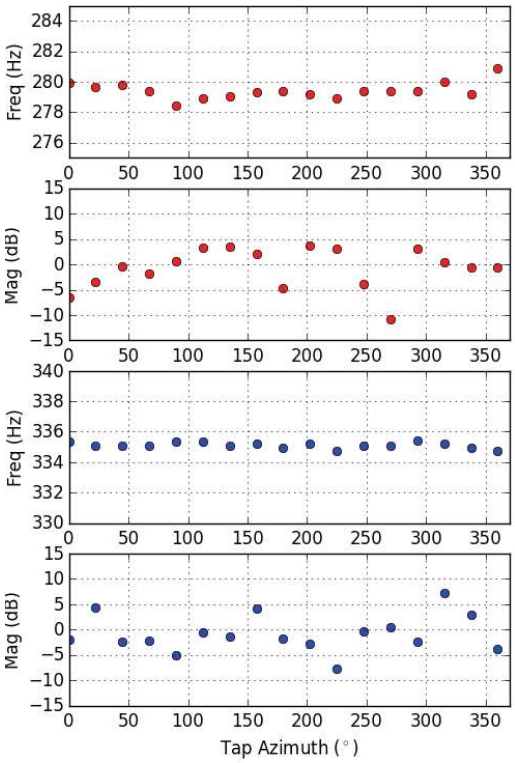

Figure 11. 10 Hz Nodal geophone: Azimuthal variation in frequency and magnitude for resonances at 279 Hz, red and 335 Hz, Blue.

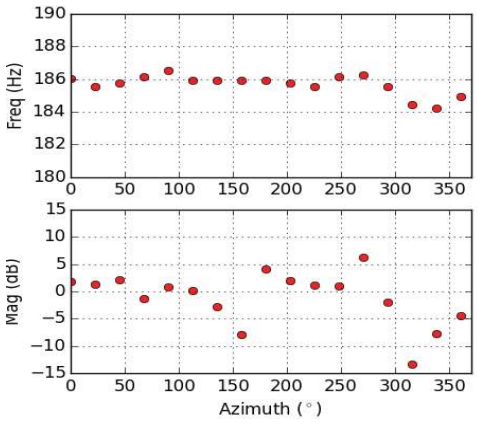

Figure 12. 5 Hz Nodal geophone: Azimuthal variation in frequency and magnitude for resonance at 186 Hz.

In an effort to focus the energy more strongly on the spurious resonance, we further narrowed the sweep (50-220 Hz). Again we found no obvious evidence of spurious behaviour stimulated by seismic waves. Interestingly, on the far-offset 5 Hz node we detected a possible anomaly, associated with the airblast arrival. Figure 13 shows spectra calculated for 0.4s windows on either side of the airblast event.

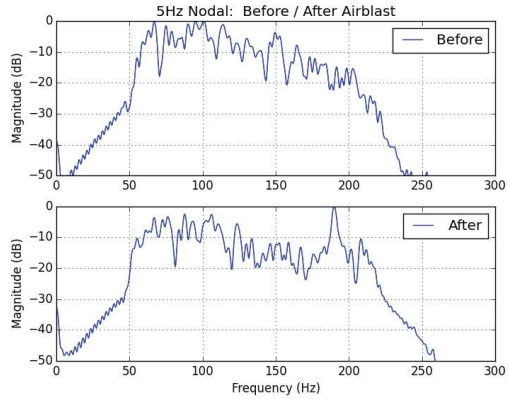

Figure 13. Far-offset 5 Hz nodal sensor: Spectra for a 0.4s window before and after airblast event. Vibroseis sweep: 50-220 Hz.

On the lower plot, the anomalous peak near 190 Hz correlates with the expected spurious resonance for the 5 Hz sensor. The airblast provides a relatively broadband horizontally-orientated impulse, which is more likely to excite the 5 Hz sensor.

CONCLUSIONS

The tap-test methodology described here accurately reveals the frequencies of spurious geophone resonances. An important component is the subtraction of an appropriately matched noise spectrum. This process effectively attenuates background noise and ambient noise peaks which might be confused with spurious events.

For all sensors tested, spurious resonance can be easily excited by vertical or side taps, although the relative strength changes. This suggests that spurious resonance could potentially arise from various seismic arrivals (P, S, surface wave). Generally, a reasonably consistent pattern is apparent for modest departure from verticality (12°). This covers the acceptable range typically seen in the field. For more radical tilts, the resonance patterns can change significantly.

Tests of a conventional 10 Hz geophone indicate a large number of spurious peaks starting around 25 times the natural frequency. The high-output nodal sensors exhibited a somewhat simpler spurious resonance pattern, with one or two dominant events. For the 10 Hz device, the lowest resonance appears to be at about 28 times the natural frequency, while for the 5 Hz device the multiplier is about 35. The improved bandwidth on these newer devices reflects continuing engineering advances over many decades. The 10 Hz node had resonances around 280, 310 and 345 Hz, which appear to vary in magnitude with azimuth of excitation. The 5 Hz node had an obvious single resonance near 186 Hz. As expected the lower-frequency device is quiet sensitive to tilt, with the resonance amplitude increasing, and resonance frequency dropping slightly (~183 Hz) for a tilt of 12°.

Tap tests provide a relatively robust impulse, and can easily excite spurious responses. The excitation delivered by field sources would often be less intense. In our field experiment, we were not able to easily excite obvious spurious response, even when vibrating through the expected anomalous frequency band. Of interest was one observation of a possible spurious response excited by horizontally travelling airblast. Additional infield experimentation is needed to further clarify the real impact of spurious geophone behaviour in field situations.

The results presented here are meant to be indicative only, and technically apply only to the specific sensors tested. Large-scale testing is needed to properly assess variability of resonance behaviour within each product line.

The methodology illustrated here provides a pragmatic basis for quantitative understanding of the spurious resonance of particular geophones. Such information is critical for the design and quality control of broadband seismic surveys.

REFERENCES

Boll S.F.,1979, Suppression of acoustic noise in speech using spectral subtraction: IEEE Acoustics, Speech and Signal Proc., **27**, 113-120.

Chen S. J., and Dalton, C., 1983, Theoretical and experimental approaches to the geophone spurious frequency: Geophysical Prospecting, **31**, 574-590.

Erturk, M., Bottomley, P., and El-Sharkawy, A., 2013, Denoising MRI Using Spectral Subtraction: IEEE, Biomedical Engineering., **60**, 1556-1562.

Faber, K., and Maxwell, P., 1997, Geophone spurious frequency: What is it and how does it affect seismic data quality: Canadian J. Exploration Geophysics, **33**, 46-54.